Investigation of Application for Surface Plasma Resonance

Jin Li
Department of Physics
University of Washington
Seattle WA

Submitted in partial fulfillment of the requirements for the
Master's degree in Physics

Project Advisor: Larry Sorensen

1 Introduction

Surface plasmon resonance (SPR) was first observed and discussed by R.W. Wood, who discovered the effect of surface plasmons on the intensity of light diffracted from metal grating in 1902 and Sommerfeld proposed surface plasmon waves as solutions to Maxwell's equations in 1909. There were two important revolutions in history. The first revolution, which was in the application of SPR methods in physical science, was stimulated by the invention in 1968 of practical methods to generate and study surface plasmons in uniform metal films by Otto and by Krechman and Raether. The second revolution, which was in the application of SPR methods in the biological sciences, was stimulated by the invention in 1988 of surface plasmon microscopy, which allows parallel, high-throughput SPR measurements with high-spatial resolution.

I have worked on the SPR experiments since summer quarter, 2000, when I was in Professor Sorensen's class, 'Selected Topics of Application Physics.' I became interested in SPR experiments and applications because there are many physics theories and fine measurements involved. I selected SPR as my independent research project from several options after Professor Sorensen told me about the new SPR applications in biological technology.

In this paper, I will present my study of SPR on multi-layer samples including prisms, gold, DNA, and protein layers. I begin by introducing DNA, SPR and deriving dispersion equations for surface plasma in multi-layered structures. I then present a SPR MathCAD program, which will help to allow for understanding of the basis for the SPR theories and experiments. Finally, I give a discussion of the experimental results and explain them in the framework of theory and calculations.

1.1 What is SPR?

Surface Plasmon Resonance (SPR) is a quantum optical-electrical phenomenon. The SPR technique has emerged as a powerful technique for a variety of chemical and biological applications. It can be used as the basis for a sensor, which is capable of sensitive and quantitative measurement of a broad spectrum of chemical and biological entities. It offers a number of important practical advantages over current analytical techniques.

Surface plasmons are collective oscillations of free electrons in a metallic film. Under appropriate conditions, the plasmons can be excited with light, which results in the absorption of light. Because the resonate condition is extremely sensitive to the refractive

index of the medium adjacent to the metal film, adsorption of molecules on the metallic film or conformation changes in the adsorbed molecules can be accurately detected.

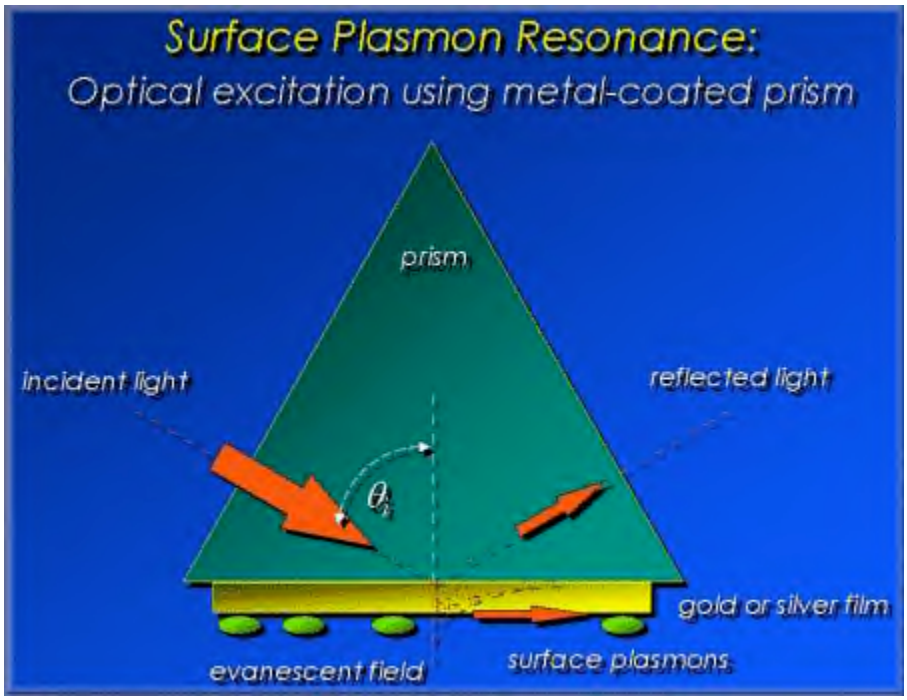

We shine a light beam perpendicular to the flat surface of a prism and increase the angle of incidence. At a critical angle, the refractive light will be exactly parallel to the flat surface. Beyond that angle, the beam will be reflective inside the prism and no light will pass through. This phenomenon is called Total Internal Reflection (TIR). Although no light actually passes out of the prism in TIR, the electric field of the photons extends about a quarter of a wavelength beyond the reflecting surface.

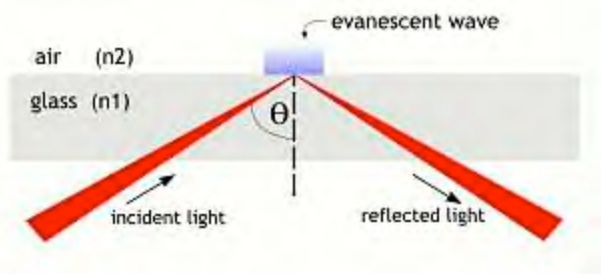

If we now have a thin gold film on the flat surface of the prism, the electric constellations in the gold surface if the energy is just right. When this happens, the incident photons are converted into surface plasmons: You have surface plasmon resonance and the light is no longer totally reflected. The incident photons are transformed into plasmons in the gold surface. Light and electric density waves have momentum as well as energy, and both must be conserved in the photon-to-plasmon transformation. Resonance occurs when the momentum of the incoming photons is equal to the plasmon momentum. This is called “wave vector coupling”.

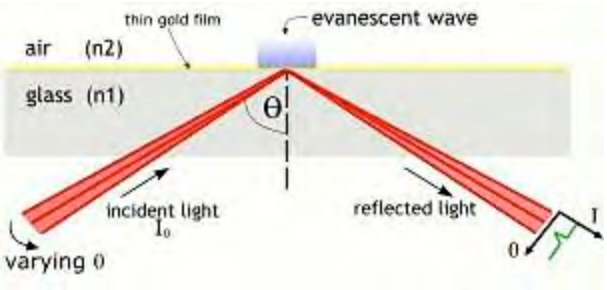

The momentum for photons and plasmons is a vector. For the SPR it is only the vector component of the momentum parallel to the surface that matters. Resonance occurs at the specific angle of incident light where the plane-parallel components of the momentums for the photon and the plasmon are equal.

1.2 What is DNA?

The fundamental chemical building block of deoxyribonucleic acid (DNA) is the nucleotide. A nucleotide consists of three parts: (1) a nitrogen-containing pyrimidine or purine base, (2) a deoxyribose sugar, and (3) a phosphate group that acts as a bridge between adjacent deoxyribose sugars.

The diameter of the DNA helix is 2 nm and the vertical rise per base pair is 0.34 nm Ho89]. A DNA molecule is composed of two unbranched polynucleotide chains (strands) that wind about each other into a structure called a double helix. The structure of the DNA helix is stabilized by van der Waals forces, hydrogen bonds between complementary organic bases (a base pair), and hydrophobic interactions between the nitrogenous bases and the surrounding sheath of water. The alternating sugar-phosphate groups in each DNA strand form the so-called *backbone* of DNA, and they also confer a directionality. Suppose the double helical structure of DNA could be unwound and both strands of DNA laid side-by-side. Then, the sugar-phosphate linkages in one strand would proceed from the 5′ to 3′ carbon, and the sugar-phosphate linkages in the other strand would proceed in 3′ to 5′ direction.

The helical structure described by Watson and Crick, called B-DNA, is only one of several possible conformations. Other DNA conformations use the same nucleotides and molecular bonds, but the three-dimensional structure of the helix is different. At least six different DNA conformations (designated A, B, C, D, E, and Z) have been identified, but only the A, Z, and B conformations are found in nature. B-DNA is the most common form of DNA found in living organisms. The average diameter of B-DNA is about 2.0 nm. Other DNA conformations have diameters that range from about 1.8 to 2.3 nm. The average distance between adjacent nucleotides in the same strand of DNA (the *vertical rise*) is between 0.321 to 0.337 nm. The B-DNA helix makes one full revolution approximately every 10.1 to 10.6 nucleotides.

The average mass of a base pair in DNA is about 615 dalton (Da); a dalton (Da), is equivalent to 1/12 the mass of the 12C which equals 1.66053873E-27 kg.

2 Surface Plasmon Theory

It is possible to conceive of a metal, such as silver and gold, as plasma. Certainly, a chunk of metal bears very little resemblance to plasma of a fusion reaction. The chunk of metal is easily thought of as a positive charged back ground with a relatively free-moving sea of electrons. In this electrons sea, electrons can act collectively, giving rise to waves of charge density along the surface and through the volume. The quantum of energy associated with this charge-density oscillation has been termed plasmon, analogous to the term “photon” when discussing light.

In a homogeneous and isotropic medium and with $\rho = 0$ and $j = 0$. Maxwell's equation yield:

$$\text{Laplacian of } E - \frac{\mu\cdot\varepsilon}{c^2}\cdot\frac{d^2}{dt^2}E = 0 \quad \text{and} \quad \text{Laplacian of } H - \frac{\mu\cdot\varepsilon}{c^2}\cdot\frac{d^2}{dt^2}H = 0 \tag{2.1}$$

Where ρ is electron charge density, j is current, c is the speed of light, μ is magnetic permeability, and ε is the permittivity. Solution to those wave equations in (2.1) is plane waves $A\cdot\exp(-i(k\cdot r - \omega\cdot t))$ of frequency ω and wave vector **k**, with $k^2 = \frac{\omega^2}{c^2}\cdot\mu\cdot\varepsilon$ (2.2)

We assume the magnetic permeability, $\mu = 1$, i.e., that all media under consideration are non-magnetic.

Consider the application of these equations to the region about the plane boundary of two media as shown in figure 1. The dielectric constant of medium 1 is assumed real and positive. For the time being assume ε_2 to be real, but make no assumption about its sign.

$Z > 0$ $\quad \varepsilon 1 > 0$ $\quad$ medium 1

$Z < 0$ $\quad \varepsilon 2 < 0$ $\quad$ medium 2

Figure 2.1.1: The surface of two optical mediums.

Consider the following possible solution to the wave equations:

$Z \geq 0$

$$E_x = E_0\cdot\exp(k\cdot x - \omega\cdot t)\cdot\exp(k\cdot x - \omega\cdot t)\cdot\exp\left[-\left\{k^2 - \varepsilon_1\cdot\frac{\omega^2}{c^2}\right\}^{\frac{1}{2}}\cdot z\right] \tag{2.3}$$

$$E_y = 0 \tag{2.4}$$

$$E_z = i\cdot k\cdot E_0\cdot\left\{k^2 - \varepsilon_1\cdot\frac{\omega^2}{c^2}\right\}^{-\frac{1}{2}}\cdot\exp(k\cdot x - \omega\cdot t)\cdot\exp\left[-\left\{k^2 - \varepsilon_1\cdot\frac{\omega^2}{c^2}\right\}^{\frac{1}{2}}\cdot z\right] \tag{2.5}$$

$Z \leq 0$

$$E_x = E_0\cdot\exp(k\cdot x - \omega\cdot t)\cdot\exp(k\cdot x - \omega\cdot t)\cdot\exp\left[\left\{k^2 - \varepsilon_1\cdot\frac{\omega^2}{c^2}\right\}^{\frac{1}{2}}\cdot z\right] \tag{2.6}$$

$$E_y = 0 \tag{2.7}$$

$$E_z = -i\cdot k\cdot E_0\cdot\left\{k^2 - \varepsilon_1\cdot\frac{\omega^2}{c^2}\right\}^{-\frac{1}{2}}\cdot\exp(k\cdot x - \omega\cdot t)\cdot\exp\left[\left\{k^2 - \varepsilon_1\cdot\frac{\omega^2}{c^2}\right\}^{\frac{1}{2}}\cdot z\right] \tag{2.8}$$

These solutions (called surface waves because they propagate along the surface z = 0) satisfy the wave equations and provided that certain constraints are met, will also satisfy the boundary condition imposed by Maxwell's equations. First note that for those solutions to be physically sensible, their amplitude must decay exponentially away from the boundary, which will be the case if

$$\left(k^2 - \varepsilon_1 \cdot \frac{\omega^2}{c^2}\right)^{\frac{1}{2}} > 0 \quad \text{and} \quad \left(k^2 - \varepsilon_2 \cdot \frac{\omega^2}{c^2}\right)^{\frac{1}{2}} > 0 \tag{2.9}$$

The boundary condition require continuity of the tangential components of **E** and **H** at z = 0. For **E** this is satisfied by choice of constants (E_0), and for **H**, we get the result:

$$\varepsilon_1 \cdot \left(k^2 - \varepsilon_2 \cdot \frac{\omega^2}{c^2}\right)^{\frac{1}{2}} = -\varepsilon_2 \cdot \left(k^2 - \varepsilon_1 \cdot \frac{\omega^2}{c^2}\right)^{\frac{1}{2}} \tag{2.10}$$

This can be only true if $\varepsilon 2 < 0$, solving for k from (2.10), we obtain:

$$k^2 = \frac{\varepsilon_1 \cdot \varepsilon_2}{\varepsilon_1 + \varepsilon_2} \cdot \frac{\omega^2}{c^2} \qquad \text{or} \qquad \omega^2 = (c \cdot k)^2 \cdot \left\{\frac{1}{\varepsilon_1} + \frac{1}{\varepsilon_2}\right\} \tag{2.11}$$

This result tells us that we must have $-\varepsilon_2 > \varepsilon_1$ for k not to be pure imaginary. So far as the surface waves exist, we must have $\varepsilon_2 < 0$ and $-\varepsilon_2 > \varepsilon_1$

We have assumed that ε_2 is real. For many metals the dielectric constant has an imaginary part, resulting in attenuation in the direction of propagation.

For now assume that medium 1 is air ($\varepsilon_1 = 1$) and that medium 2 is a metal. The free electron gas model for metal gives refraction index.

$$n(\omega)^2 = \varepsilon(\omega) = 1 - \left(\frac{\omega_p}{\omega}\right)^2 \tag{2.12}$$

$$\omega_p = e \cdot \sqrt{\frac{N \cdot f}{m \cdot \varepsilon_0}} \tag{2.13}$$

Where ω_p is the plasma frequency, f is the number of free electrons per molecule and N is the number of molecules per unit volume. The dispersion relation for surface waves now looks like

$$\omega^2 = (c \cdot k)^2 \cdot \left\{\frac{1}{\varepsilon_1} + \frac{1}{\varepsilon_2}\right\} = (c \cdot k)^2 \cdot \left[1 + \left[\frac{1}{1 - \left(\frac{\omega_p}{\omega}\right)^2}\right]\right] \tag{2.14}$$

We can solve this equation and get

$$\omega^2 = \frac{\left(\omega_p\right)^2}{2} + (c\cdot k)^2 - \left[\frac{1}{4}\cdot\left(\omega_p\right)^4 + (c\cdot k)^4\right]^{\frac{1}{2}} \qquad (2.15)$$

See Appendix # ?

For small k: $(\frac{c\cdot k}{\omega_p} << 1)$ $\qquad \omega^2 = (c\cdot k)^2\cdot\left[1 - \frac{1}{2}\cdot\left\{\frac{\omega_p}{2}\right\}^2\right]$ (2.16)

For large k: $(\frac{c\cdot k}{\omega_p} >> 1)$ $\qquad \omega^2 = \frac{\left(\omega_p\right)^2}{2}\cdot\left[1 - \frac{1}{4}\cdot\left\{\frac{c\cdot k}{\omega_p}\right\}^2\right]$ (2.17)

For all values of k>0, the dispersion curve for surface plasmons propagation along the metal-air boundary lies to the right of the dispersion curve for electromagnetic waves in air $\omega = c*k$.

2.1 Two Layer Case

In the two layer case, surface charges are produced which satisfy Maxwell's equations governing the boundary conditions on the normal component of the electric field between two media.

In figure 2.1.2, the straight line represents the dispersion curve for plane waves traveling in the x-direction inside the upper dielectric medium like in prism. The curved line represents the SPW dispersion curve in the two-layer case.

Because these dispersion curves do not intersect, it is not possible to match the frequency (ω) and wave vector (k) of the surface plasmons to the frequency and wave vector of incident electromagnetic radiation in air. (This is why those Surface Plasmons are called non-irradiative). (MathCAD calculations can be found in Appendix 2.1.2)

The boundary conditions only result in physically valid solution for TM polarization. Consequently, TE polarized SPW do not exist. This is not only true for the two-layer case, but applies to a structure with any number of layers. It should be pointed out that if the SPW is to be excited optically, the incident radiation must also be TM polarized, in order to couple with the TM polarized SPW.

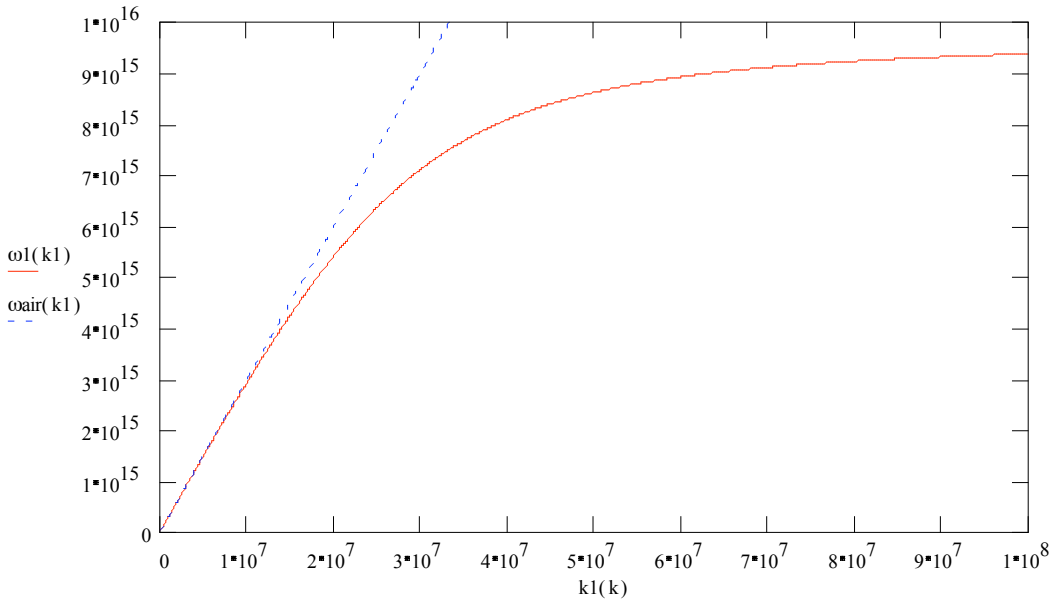

Figure 2.1.2 Dispersion curves for two-layer case. The slop of the straight line is c/N_{air}

2.2 Three Layer Case

If for a given ω, the k of light incident on the metal- air boundary is increased, the dispersion curves will intersect. Physically, this can be accomplished by passing the incident light through a medium, such as glass, on which a metal film is deposited. The glass has the effect of multiplying the wave vector by N_{glass}, the index of refraction of glass. And the thin film allows some of the incident light to be transmitted through to the metal-air boundary, where the surface plasma are excited. Actually it is the wave vector component of the surface incident light parallel to the boundary that must be matched to the surface plasma wave vector by varying incident angle θ.

$$k \cdot N_{glass} \cdot \sin\left\{\theta_i\right\} = k_{sp} \quad \text{again} \quad \frac{\omega}{k} = c \cdot \left\{\frac{\varepsilon_1 \cdot \varepsilon_2}{\varepsilon_1 + \varepsilon_2}\right\} \tag{2.18}$$

Where $k = \omega/c$, N_{glass} is refractive index, θ_i is the angle of incidence for SPR

In Figure 2.2.1, the straight line represents the dispersion curve for plane waves in the prism. These dispersion curves do intersect, therefore, it is possible to match the ω and k of the surface plasmons to the frequency and wave vector of incident electromagnetic radiation in air, which means SPR may be generated in this case. (MathCAD calculations can be found in Appendix 2.1.2)

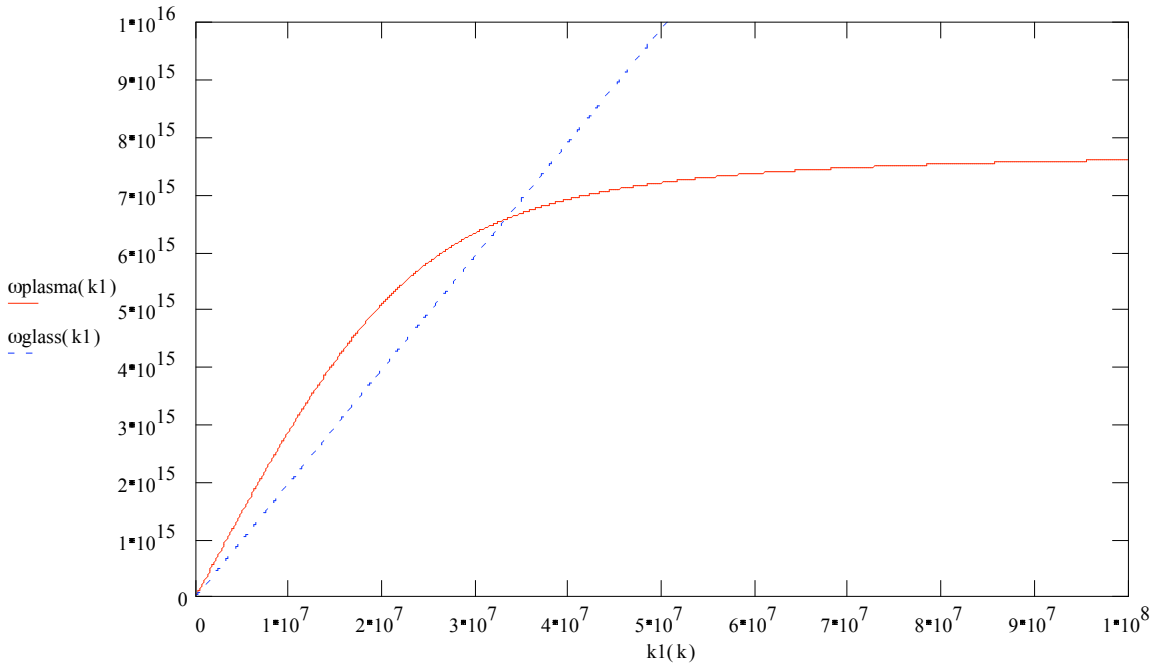

Figure 2.2.1 Dispersion curves for three-layer case. The slope of the straight line is c/N_{glass}

3 Modeling Surface Plasmon Resonance

3.1 General Equations for N Layer system

In this general case, with N-1 surface of discontinuity at $z = z_k$ (k=1,2…N-1), there is a matrix Mk characteristic of each space $z_{k-1} < z < z_k$ and for the final region $z < z_{n-1}$. The tangential fields at the first boundary, $z = z_1 = 0$, are related to those at the final boundary, $z < z_{n-1}$, by:

$$\begin{pmatrix} U_1 \\ V_1 \end{pmatrix} = M_2 \cdot M_2 \ldots\ldots M_{N-1} \cdot \begin{pmatrix} U_{N-1} \\ V_{N-1} \end{pmatrix} \qquad (3.1)$$

We defined:

$$M_2 \cdot M_3 \ldots\ldots M_{N-1} = M \qquad (3.2)$$

So:

$$\begin{pmatrix} U_1 \\ V_1 \end{pmatrix} = M_2 \cdot M_3 \ldots M_{N-1} \cdot \begin{pmatrix} U_{N-1} \\ V_{N-1} \end{pmatrix} = M \cdot \begin{pmatrix} U_{N-1} \\ V_{N-1} \end{pmatrix} \qquad (3.3)$$

Where M is the characteristic matrix of the plane bounded layers as a group and U_k and V_k are the tangential components of the field amplitudes at the boundary k, $U_k = H_y$ and $V_k = E_x$. The characteristic matrix for the j_{th} layer is given for TM polarization by

$$M_j = \begin{bmatrix} \cos(\beta_j) & -\frac{i}{q_j}\cdot\sin(\beta_j) \\ -i\cdot q_j\cdot\sin(\beta_j) & \cos(\beta_j) \end{bmatrix} \tag{3.4}$$

Where $q_j = \sqrt{\frac{\mu_j}{\varepsilon_j}}\cdot\cos(\theta_j)$ $\beta_j = \frac{2\cdot\pi}{\lambda}\cdot n\cdot d\cdot\cos(\theta_j)$ $\cos(\theta_j) = \sqrt{1-\left(\frac{n_1}{n}\cdot\sin(\theta_j)\right)^2}$ (3.5)

From Equation (3.3), we can derive the reflection and transmission coefficients of the stack

$$r_{11} = \frac{(m_{11}+m_{12}\cdot q_N)\cdot q_1 - (m_{11}+m_{22}\cdot q_N)\cdot q_N}{(m_{11}+m_{12}\cdot q_N)\cdot q_1 + (m_{11}+m_{22}\cdot q_N)\cdot q_N} \tag{3.6}$$

$$t_{11} = \frac{2\cdot q_1}{(m_{11}+m_{12}\cdot q_N)\cdot q_1 + (m_{11}+m_{22}\cdot q_N)\cdot q_N} \tag{3.7}$$

In those equations, the $m_{i,j}$ is the elements of the matrix M given by equation (3.3), which is characteristic of the stratified medium.
From the above equations,

$$R_{TM} = \left[\frac{(m_{11}+m_{12}\cdot q_N)\cdot q_1 - (m_{11}+m_{22}\cdot q_N)\cdot q_N}{(m_{11}+m_{12}\cdot q_N)\cdot q_1 + (m_{11}+m_{22}\cdot q_N)\cdot q_N}\right]^2 \tag{3.8}$$

3.2 Computer Modeling

It is assumed in Fig 3.1 that a plane wave is incident on the structure from the left, and each layer in the structure is isotropic, but can in general have a complex index of refraction. The interfaces between each layer are assumed to be perfectly smooth. For the case of TM polarization the transmission and reflection coefficients for the electric fields can be derived and found to be

$$R_{TM} = \left[\frac{(m_{11}+m_{12}\cdot q_N)\cdot q_1 - (m_{11}+m_{22}\cdot q_N)\cdot q_N}{(m_{11}+m_{12}\cdot q_N)\cdot q_1 + (m_{11}+m_{22}\cdot q_N)\cdot q_N}\right]^2$$

Where $q_1 = \frac{1}{n_1}\cdot\cos(\theta_j)$ $q_N = \frac{1}{n_N}\cdot\cos(\theta_j)$ are the wave impedances of the initial and final layer in the structure, respectively. The wave impedances relate the electric and magnetic fields in each layer. The matrix coefficients are given by $M_2\cdot M_3 \ldots\ldots M_{N-1} = M$

Where

$$M_N = \begin{bmatrix} \cos\left(\beta_N\right) & -\frac{i}{\left(q_N\right)_{m,j}} \cdot \sin\left(\beta_N\right) \\ -i \cdot q_N \cdot \sin\left(\beta_N\right) & \cos\left(\beta_N\right) \end{bmatrix} \tag{3.9}$$

And q_N d_N k_N and θ_N are the wave impedance, thickness, wave vector, and angle of propagation in the nth layer, respectively. The angle of propagation in the nth layer can be determined as a function of the angle of incidence in the first layer using:

$$\cos\left(\theta_N\right) = \sqrt{1 - \left\{\frac{n_1}{n_N} \cdot \sin(\theta)\right\}^2} \tag{3.10}$$

There is a separate matrix for each of layers, from layer two to layer m in Fig
The matrix coefficients for the nth layer are given by:

$$M = \begin{pmatrix} m_{11} & m_{12} \\ m_{21} & m_{22} \end{pmatrix} \tag{3.11}$$

The calculation has been implemented as a computer program using MathCAD software. (The code for the calculation can be found in Appendix 3.2.2)

3.2.1 Compare MathCAD curves with the curves in an article

To verify this MathCAD program, I modified the MathCAD program to fit curves for silver films with carbon coatings of different thickness d_c from I. Pockand, surf. Sci. 72, 577 (1978) and found that those matched very well.
The strong absorption of carbon causes the rapid broadening of the resonance, even for very small d_c (of several atomic layers). The half width increase and depth change for carbon coated silver films are accompanied by the expected large shift of the resonance angle to greater values due to the high real part of the carbon dielectric function.
(The carbon dielectric function given in ref. $\varepsilon_c = 3.86 + 457i$)

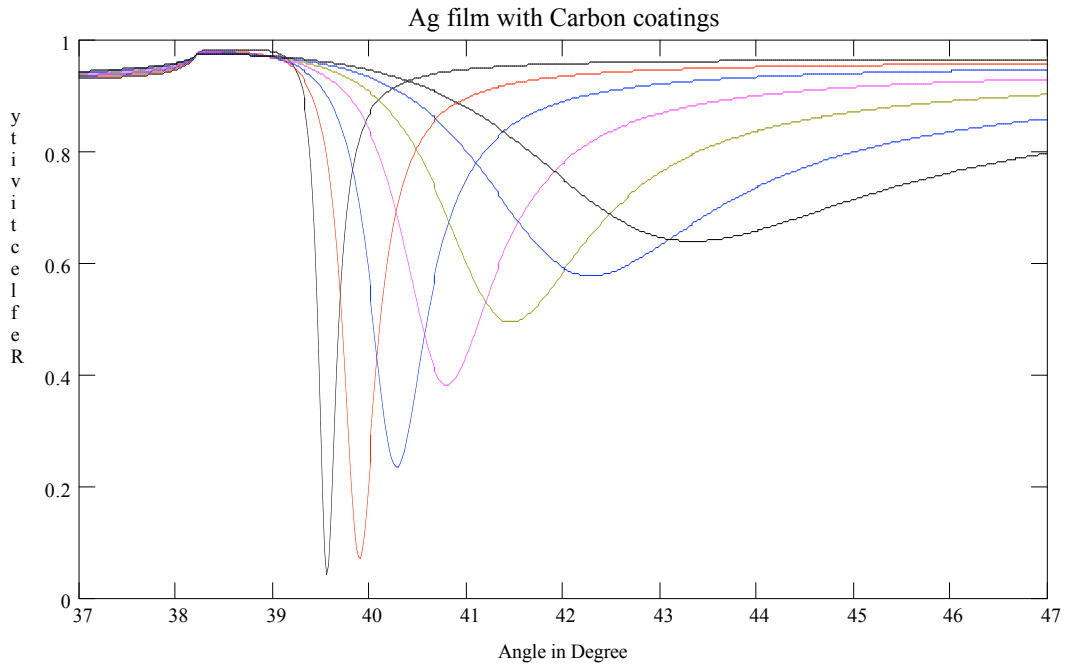

Figure 3.2.5 Resonance curves for silver films with carbon coating of various carbon thicknesses.

3.3 Analysis from Computer Modeling

3.3.1 Total Internal Reflection

The light will be totally reflected if there is no gold or silver film on the back surface of the prism. Rays from the object that make increasingly larger angles of incidence with the interface must, by Snell law, refract at increasingly larger angle. A critical angle of incidence θ is reached when the angle of refraction reach 90 degree. Thus from Snell's law:

$$\theta = \operatorname{asin}\left\{\frac{nair}{nglass}\right\}\cdot\frac{180}{\pi} = 41.3$$

Which matches the data from the MathCAD model shown in below:

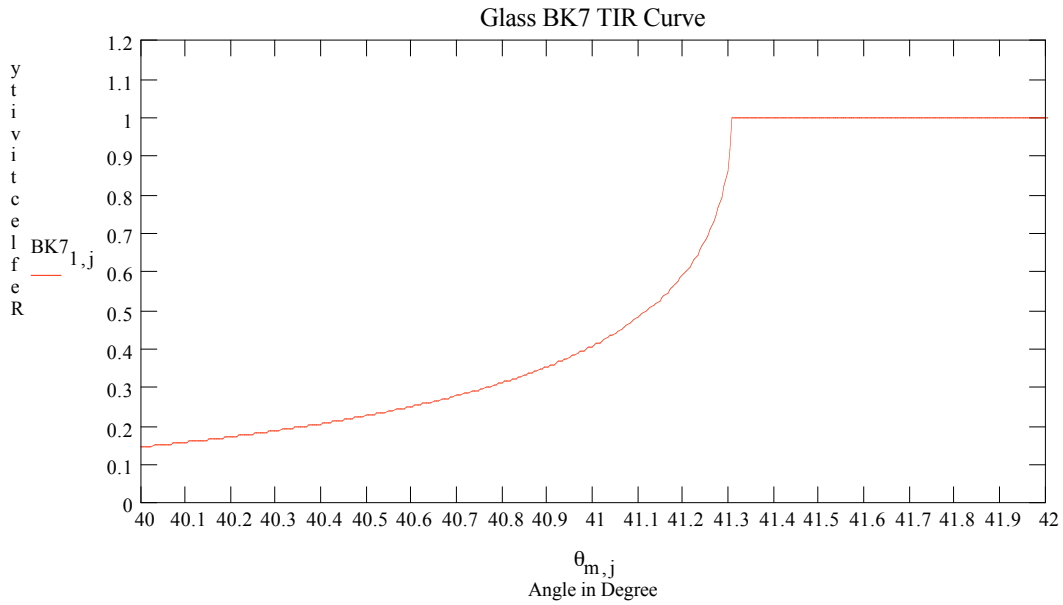

Figure 3.3.1: Reflected light intensity as a function of the angle of incidence θ. (MathCAD model can be found in Appendix 3.2.1)

3.3.2 Optimize the gold thickness

The different gold thickness are represented by different curves, which are shown below and the best thickness, 50 nm gold film, has the lowest R_{min}

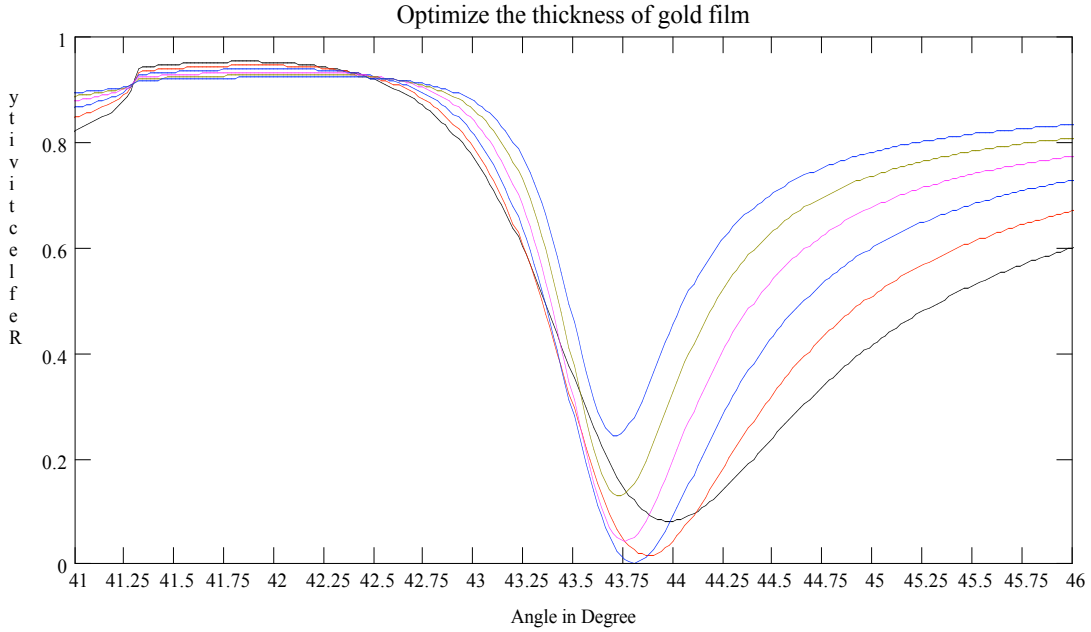

Figure 3.3.2 MathCAD plot for a system with λ = 633 nm, a BK7 prism (n = 1.151) and the thickness of the gold film for each curve, from 40 nm (bottom curve from right), 45, 50 (the curve with the lowest R_{min}), 55, 60, 65 nm (top from right). The index of refraction of the gold film is 0.1726 + 3.4218i. (MathCAD model can be found in Appendix 3.2.2)

3.3.3 Optimize the real part index of refraction of gold film

Figure 3.3.3. shows the effect of varying the real part of the index of refraction of the bulk dielectric, n_{dr}. It can be seen from this graph that varying n_{dr} strongly affects the parameters $\Delta\theta$ and R_{min}. If the exact relationship between n_{dr} and $\Delta\theta$, or n_{dr} and R_{min} is known, it should be possible to determine an unknown n_{dr} by measuring $\Delta\theta$ or R_{min}, assuming that n_{di} remains constant.

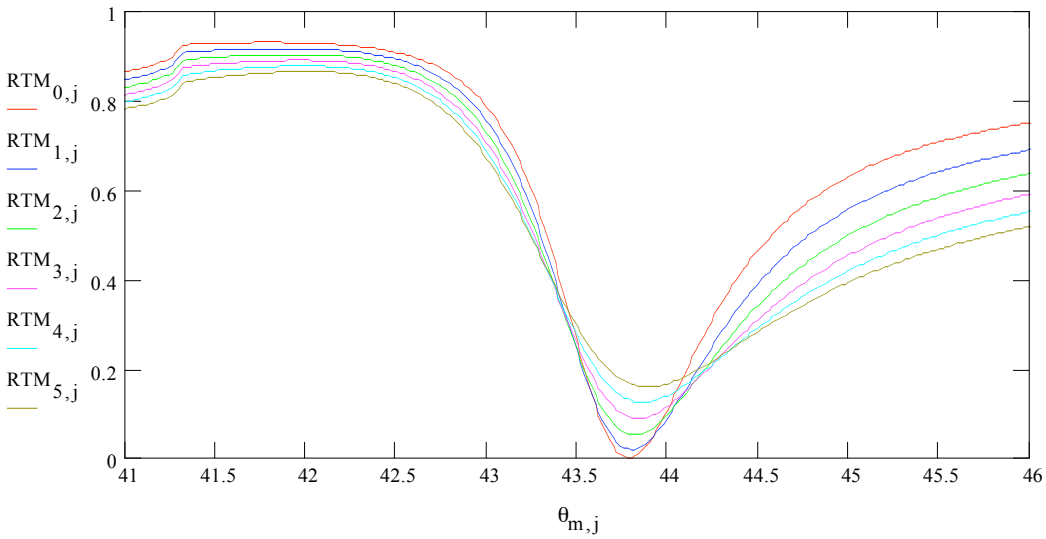

Figure 3.3.3 MathCAD plot for a system with λ = 633 nm, a BK7 prism (n = 1.151) and a 50 nm thick gold film. The real part of the index of refraction of the dielectric varies for each curves, from 0.15 (top curve from right), 0.20, 0.25, 0.30, 0.35, 0.40 (bottom curve from right). The imaginary part of the dielectric's index is 3.4218i in each case.

3.3.4 Optimize the Imaginary part index of refraction of gold film

Figure 3.3.4. shows the effect of varying the imaginary part of the index of refraction of the bulk dielectric, n_{di}. It can be seen from this graph that varying n_{di} strongly affects the parameters θ_{sp}. As the real part of the bulk dielectric increases, θ_{sp} shifts to larger angle.

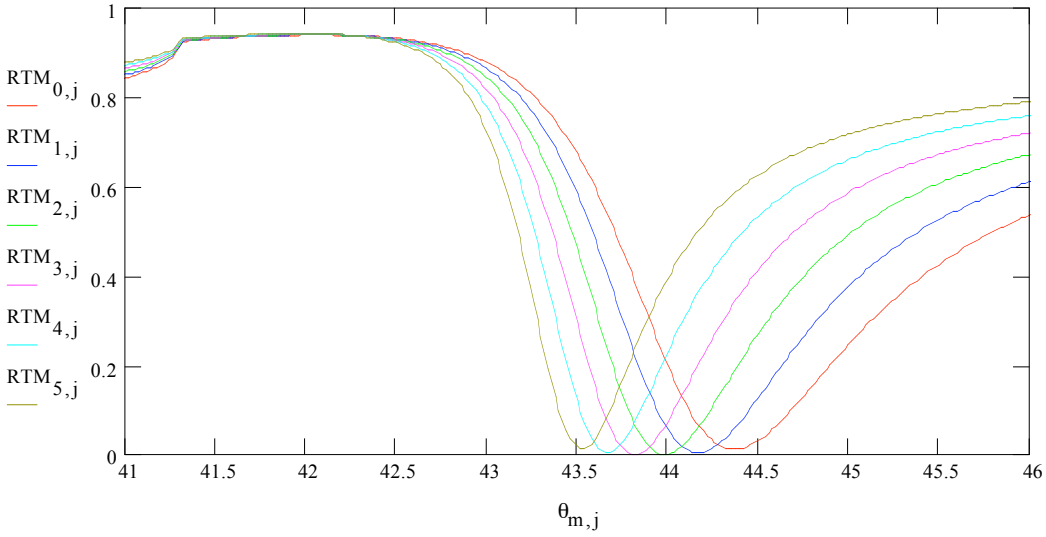

Figure 3.3.4 MathCAD plot for a system with λ = 633 nm, a BK7 prism (n = 1.151) and a 50 nm thick gold film. The imaginary part of the index of refraction of the dielectric varies for each curves, from 3.1 (top curve from right), 3.2, 3.3, 3.4, 3.5, 3.6 (bottom curve from right). The imaginary part of the dielectric's index is 01726 in each case.

3.3.5 Compare gold film and Silver film

If we now have a thin gold film on the flat surface of the prism, we get surface plasmon resonance and the light is no longer totally reflected. Compare gold (solid line) and silver film (dash line) on glass prism, both films are 50 nm thick and light source is 632.8 nm, we can see that the gold film curve is sharper, which means gold film is more sensitive than silver film in SPR experiment.

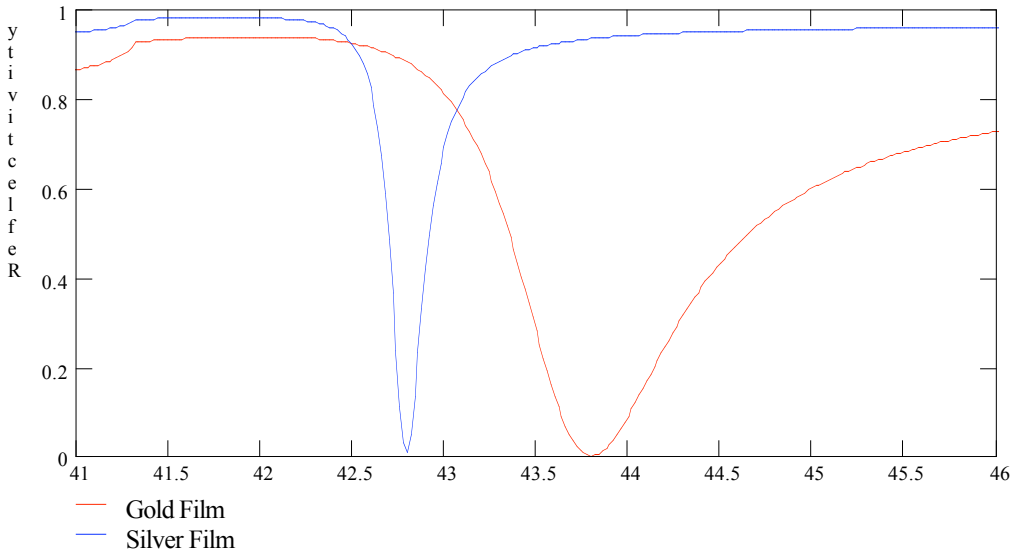

Figure 3.3.5 2 MathCAD plot for a system with λ = 633 nm, a BK7 prism (n = 1.151). The curve on right shows that gold film which thickness is 50 nm and the index of refraction of the gold film is 0.1726 + 3.4218i. The curve on left represents that silver film which thickness is 50 nm and the index of refraction of the gold film is 0.064 + 4.289i (MathCAD model can be found in Appendix 3.2.5)

3.3.6 The Sensitivity of DNA index Changes

SPR is detected by measurement of the intensity of the reflected light. At the SPR angle a sharp decrease or 'dip' of intensity is measured. The position of the SPR angle depends on the refractive index in the substance with a low-refractive index close to the sensing surface. The refractive index near the sensor surface changes because of binding of macromolecules to the surface. As a result, the SPR angle will change according to the amount of bound macromolecules. There is a linear relationship between the amount of bound material and the shift of the SPR angle.

Scanning mirror biosensors measure the SPR angle shift in millidegrees as a response unit to quantify the binding of macromolecules to the sensor surface. The response also depends on the refractive index of the bulk solution. A change of 120 millidegrees represents a change in surface protein coverage of approximately 1 ng/mm^2, or in bulk refractive index of approximately 10^{-3}.

SPR parameter	Equivalent value
SPR angle shift	120 millidegrees
Change in protein surface concentration	1 ng/mm^2
Change in bulk refractive index	0.001

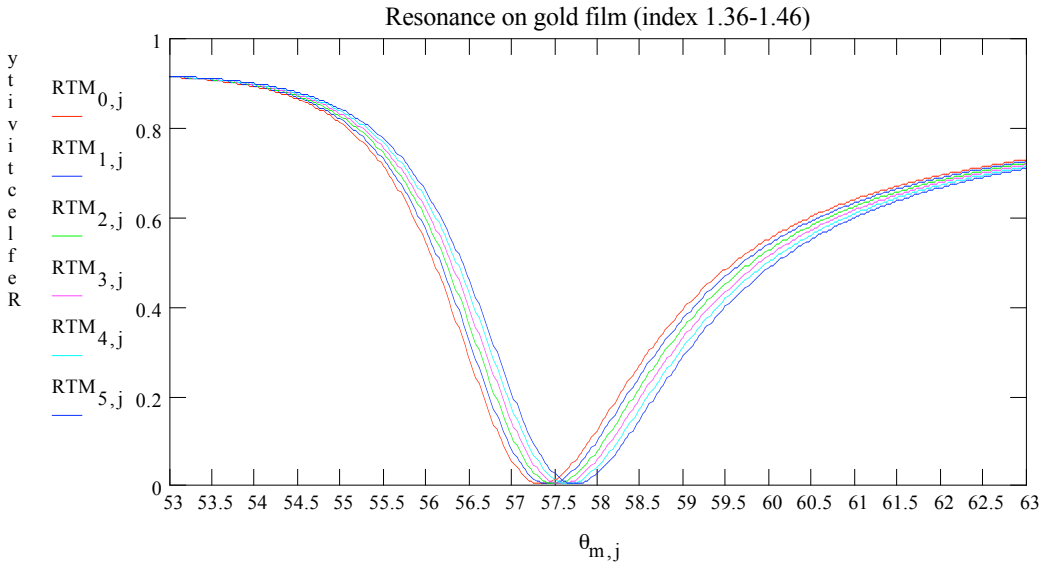

Figure 3.3.4: The key how SPR works is the resonance is very sensitive to optical index changes. The experiment is good for measuring 120 millidegrees angle change, which can be interpreted to 0.001 reflective index changes.
(MathCAD model can be found in Appendix 3.2.4)

4 Experiment

4.1 Glass (BK7)

4.2 Glass and adhesion layer

4.2 Glass, adhesion layer and Au layer

4.3 Glass, adhesion layer, Au layer and protective (oxide) layer

4.4 Glass, adhesion layer, Au layer, protective (oxide) layer and silane

4.5 Glass, adhesion layer, Au layer, protective (oxide) layer, silane and DNA

4.6 Glass, adhesion layer, Au layer, protective (oxide) layer, silane, DNA and protein

4.7 Compare Silver film experiment Data with MathCAD Model

After studied the function of the complex index of reflection, we knew that the imaginary part of the index shifts the angle of minimum reflective and the real part of the index changes the depth and width of the curve. The thickness moves both the depth and the resonance angle. In Figure 7, we plotted reflective curve from a silver film on a BK7 prism by using a 633 nm laser and fitted with a MathCAD model curve. We found that the best fit was at n = 0.086 + 3.89i and 49.5 nm thickness, which is close to the offical index n = 0.064 + 4289i.

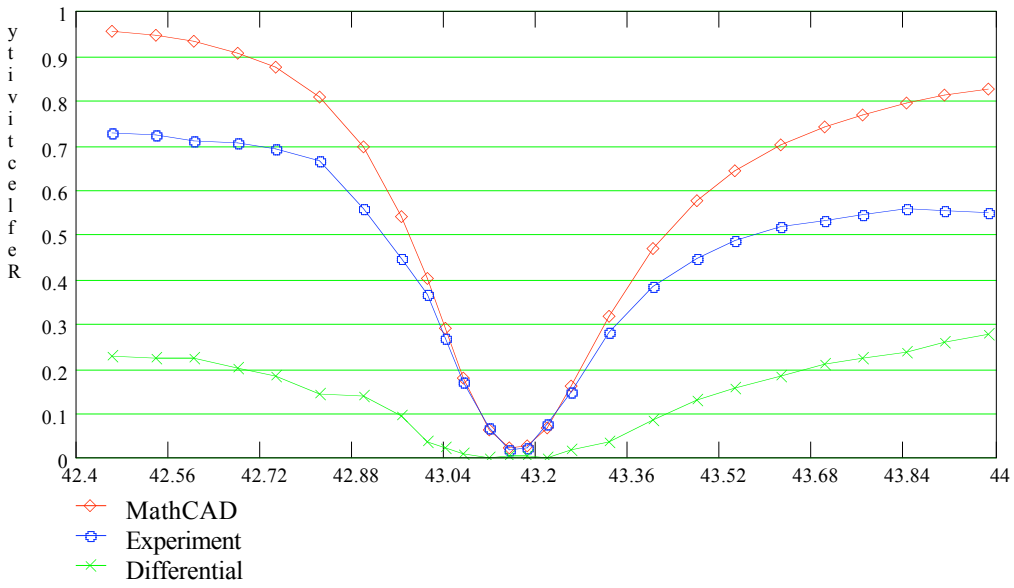

Figure 4.7.1 Reflective curves from a silver film on a BK7 (n = 1.151 at 633 nm). Diamond curve is from MathCAD model, o-curve is from experiment and the x-curve is the differential between those two curves.

5 Conclusion

6 Future work

7 Acknowledgements

8 Appendix

Appendix 2.1.2 The Dispersion Curves Calculation (Two and Three Layer Case)

$density := 10.5 \cdot 10^{3}$ $atoms := 6.0 \cdot 10^{23}$ $atomicweight := 107.9 \cdot 10^{-3}$

Refractive index in air $nair := 1.000$ Permittivity of pace $\varepsilon_0 := 8.85 \cdot 10^{-12}$

Refractive index in glass $nglass := 1.515$ Speed of light $c := 3 \cdot 10^{8}$

Charge of electron $e := 1.6 \cdot 10^{-19}$ Variable $k := 1 .. 1000$

Mass of electron $m := 9.1810^{-31}$ Wave number $k1(k) := k \cdot 10^{5}$

Number of molecules per unit $N := \frac{density \cdot atoms}{atomicweight}$ Plasma frequency $\omega p := e \cdot \sqrt{\frac{N \cdot f}{m \cdot \varepsilon_0}}$

Number of free electron per molecule $f := 1$

Plasma angular frequency $\omega sp := \sqrt{1 + \frac{1}{\left[\left\{\frac{1}{nglass}\right\}^2 - 2\right]}} \cdot \omega p$

$ksp = 3.315 \cdot 10^7$ $\omega sp = 6.564 \cdot 10^{15}$

Plasma wave number $ksp := \frac{\omega sp}{\left\{\frac{c}{nglass}\right\}}$ Limit of dispersion curve $\omega(k1) := \frac{\omega p}{\sqrt{2}}$

Dispersion curve in glass $\omega glass(k1) := \frac{c}{nglass} \cdot k1(k)$

Dispersion curve in air $\omega air(k1) := \frac{c}{nair} \cdot k1(k)$

Dispersion curve in plasma $\omega 1(k1) := \sqrt{\left[\frac{1}{2} \cdot (\omega p)^2 + (c \cdot k1(k))^2\right] - \sqrt{\frac{1}{4} \cdot (\omega p)^4 + (c \cdot k1(k))^4}}$

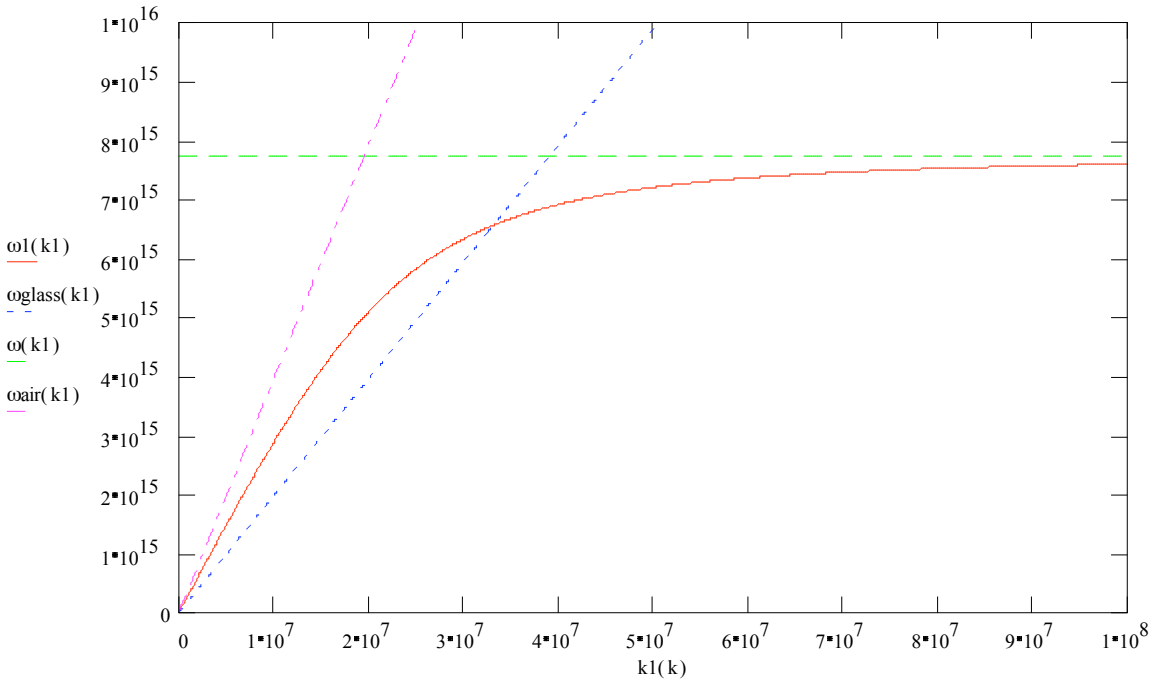

Appendix 3.2.2 Gold film SPR calculation

Wave length (m) $\lambda := 6328 \cdot 10^{-10}$ Light speed (m/s) $c := 2.9979 \cdot 10^8$

Index of Infraction

BK7 $n1 := 1.515$ Air $n6 := 1.000$ Au Film $n3 := 0.1726 + 3.4218i$ $i := \sqrt{-1}$

Thickness (m)

BK7 $d_1 := 10 \cdot 10^{-3}$ Air $d_6 := 6 \cdot 10^{-3}$

$N := 3$ $m := 0 .. N$

Gold Film Thickness (m) $d3_m := (50 \cdot m + 390) \cdot 10^{-10}$

Number of Points in Plot $M := 500$ $j := 0 .. M$

The Angler Range in Degree $Min := 40$ $Max := 50$

The angle Range in Radian $\theta_{m,j} := \left[\frac{j \cdot (Max - Min)}{M} + Min \right] \cdot \frac{\pi}{180}$

Cosine Calculation:

$$cos1_{m,j} := \sqrt{1 - \left\{ \frac{n1}{n1} \cdot \sin\left\{ \theta_{m,j} \right\} \right\}^2} \quad cos2_{m,j} := \sqrt{1 - \left\{ \frac{n1}{n2} \cdot \sin\left\{ \theta_{m,j} \right\} \right\}^2} \quad cos3_{m,j} := \sqrt{1 - \left\{ \frac{n1}{n3} \cdot \sin\left\{ \theta_{m,j} \right\} \right\}^2}$$

$$cos4_{m,j} := \sqrt{1 - \left\{ \frac{n1}{n4} \cdot \sin\left\{ \theta_{m,j} \right\} \right\}^2} \quad cos5_{m,j} := \sqrt{1 - \left\{ \frac{n1}{n5} \cdot \sin\left\{ \theta_{m,j} \right\} \right\}^2} \quad cos6_{m,j} := \sqrt{1 - \left\{ \frac{n1}{n6} \cdot \sin\left\{ \theta_{m,j} \right\} \right\}^2}$$

$$q1_{m,j} := \frac{1}{n1} \cdot cos1_{m,j} \quad q2_{m,j} := \frac{1}{n2} \cdot cos2_{m,j} \quad q3_{m,j} := \frac{1}{n3} \cdot cos3_{m,j}$$

$$q4_{m,j} := \frac{1}{n4} \cdot cos4_{m,j} \quad q5_{m,j} := \frac{1}{n5} \cdot cos5_{m,j} \quad q6_{m,j} := \frac{1}{n6} \cdot cos6_{m,j}$$

$$\beta1_{m,j} := \frac{2 \cdot \pi}{\lambda} \cdot n1 \cdot d_1 \cdot cos1_{m,j} \quad \beta2_{m,j} := \frac{2 \cdot \pi}{\lambda} \cdot n2 \cdot d_2 \cdot cos2_{m,j} \quad \beta3_{m,j} := \frac{2 \cdot \pi}{\lambda} \cdot n3 \cdot d3_m \cdot cos3_{m,j}$$

$$\beta4_{m,j} := \frac{2 \cdot \pi}{\lambda} \cdot n4 \cdot d_4 \cdot cos4_{m,j} \quad \beta5_{m,j} := \frac{2 \cdot \pi}{\lambda} \cdot n5 \cdot d_5 \cdot cos5_{m,j} \quad \beta6_{m,j} := \frac{2 \cdot \pi}{\lambda} \cdot n6 \cdot d_6 \cdot cos6_{m,j}$$

For TM polarization we get:

$$M2_{m,j} := \begin{bmatrix} \cos\left\{ \beta2_{m,j} \right\} & -\frac{i}{q2_{m,j}} \cdot \sin\left\{ \beta2_{m,j} \right\} \\ -i \cdot q2_{m,j} \cdot \sin\left\{ \beta2_{m,j} \right\} & \cos\left\{ \beta2_{m,j} \right\} \end{bmatrix}$$

$$M3_{m,j} := \begin{bmatrix} \cos\left\{ \beta3_{m,j} \right\} & -\frac{i}{q3_{m,j}} \cdot \sin\left\{ \beta3_{m,j} \right\} \\ -i \cdot q3_{m,j} \cdot \sin\left\{ \beta3_{m,j} \right\} & \cos\left\{ \beta3_{m,j} \right\} \end{bmatrix}$$

$$M4_{m,j} := \begin{bmatrix} \cos\left\{ \beta4_{m,j} \right\} & -\frac{i}{q4_{m,j}} \cdot \sin\left\{ \beta4_{m,j} \right\} \\ -i \cdot q4_{m,j} \cdot \sin\left\{ \beta4_{m,j} \right\} & \cos\left\{ \beta4_{m,j} \right\} \end{bmatrix}$$

$$M5_{m,j} := \begin{bmatrix} \cos\left(\beta5_{m,j}\right) & -\frac{i}{q5_{m,j}}\cdot\sin\left(\beta5_{m,j}\right) \\ -i\cdot q5_{m,j}\cdot\sin\left(\beta5_{m,j}\right) & \cos\left(\beta5_{m,j}\right) \end{bmatrix}$$

M is the characteristic matrix of the plane-bounded layers as a group

$$M_{m,j} := M2_{m,j}\cdot M3_{m,j}\cdot M4_{m,j}\cdot M5_{m,j}$$

f is the elements of the matrix M, which is characteristic of the stratified medium:

$$f00(m,j) := \left(M_{m,j}\right)_{0,0} \qquad f01(m,j) := \left(M_{m,j}\right)_{0,1} \qquad f10(m,j) := \left(M_{m,j}\right)_{1,0} \qquad f11(m,j) := \left(M_{m,j}\right)_{1,1}$$

We can derive the reflection coefficient of the stack

$$r_{m,j} := \frac{\left(f00(m,j) + f01(m,j)\cdot q6_{m,j}\right)\cdot q1_{m,j} - \left(f10(m,j) + f11(m,j)\cdot q6_{m,j}\right)}{\left(f00(m,j) + f01(m,j)\cdot q6_{m,j}\right)\cdot q1_{m,j} + \left(f10(m,j) + f11(m,j)\cdot q6_{m,j}\right)}$$

Reflection Ratio $RTM_{m,j} := \overline{r_{m,j}}\cdot r_{m,j}$

Appendix 3.2.4 The Sensitivity of DNA index Changes

Wave length (m) $\lambda := 6328\cdot 10^{-10}$ Light speed $c := 2.9979\cdot 10^{8}$

Index of Infraction Glass $n1 := 1.723$ Film index $n2 := 0.1726 + 3.4218i$

Sample thickness $d3 := 50\cdot 10^{-10}$ Air index $n4 := 1.333$

Glass thickness $d_1 := 1000\cdot 10^{-6}$ Film thickness $d_2 := 500\cdot 10^{-10}$

Air thickness $d_4 := 1000\cdot 10^{-6}$ $i := \sqrt{-1}$ $N := 5$ $m := 0..N$

Sample index $n3_m := 1.36 + .02\cdot m$

Number of Points in Plot $M := 500$ $j := 0..M$

The Angular Range in Degree $Min := 50$ $Max := 63$

$$\theta_{m,j} := \left[\frac{j\cdot(Max - Min)}{500} + Min\right]\cdot\frac{\pi}{180}$$

$$cos1_j := \sqrt{1 - \left\{\frac{n1}{n1}\cdot\sin\left\{\theta_{m,j}\right\}\right\}^2} \qquad cos2_j := \sqrt{1 - \left\{\frac{n1}{n2}\cdot\sin\left\{\theta_{m,j}\right\}\right\}^2}$$

$$cos3_{m,j} := \sqrt{1 - \left\{\frac{n1}{n3_m}\cdot\sin\left\{\theta_{m,j}\right\}\right\}^2} \qquad cos4_j := \sqrt{1 - \left\{\frac{n1}{n4}\cdot\sin\left\{\theta_{m,j}\right\}\right\}^2}$$

Wave Impedance

$$q1_j := \frac{1}{n1}\cdot cos1_j \qquad q2_j := \frac{1}{n2}\cdot cos2_j$$

$$q3_{m,j} := \frac{1}{n3_m}\cdot cos3_{m,j} \qquad q4_j := \frac{1}{n4}\cdot cos4_j$$

$$\beta1_j := \frac{2\cdot\pi}{\lambda}\cdot n1\cdot d_1\cdot cos1_j \qquad \beta2_j := \frac{2\cdot\pi}{\lambda}\cdot n2\cdot d_2\cdot cos2_j$$

$$\beta 3_{m,j} := \frac{2\cdot\pi}{\lambda}\cdot n3_m \cdot d3 \cdot \cos 3_{m,j} \qquad \beta 4_j := \frac{2\cdot\pi}{\lambda}\cdot n4 \cdot d_4 \cdot \cos 4_j$$

$$f00(m,j) := \frac{\left(\cos\left(\beta 2_j\right)\cdot\cos\left(\beta 3_{m,j}\right)\cdot q2_j + i^2\cdot\sin\left(\beta 2_j\right)\cdot q3_{m,j}\cdot\sin\left(\beta 3_{m,j}\right)\right)}{q2_j}$$

$$f01(m,j) := -i\cdot\frac{\left(\cos\left(\beta 2_j\right)\cdot\sin\left(\beta 3_{m,j}\right)\cdot q2_j + \sin\left(\beta 2_j\right)\cdot\cos\left(\beta 3_{m,j}\right)\cdot q3_{m,j}\right)}{\left(q3_{m,j}\cdot q2_j\right)}$$

$$f10(m,j) := -i\cdot\left(q2_j\cdot\sin\left(\beta 2_j\right)\cdot\cos\left(\beta 3_{m,j}\right) + \cos\left(\beta 2_j\right)\cdot q3_{m,j}\cdot\sin\left(\beta 3_{m,j}\right)\right)$$

$$f11(m,j) := \frac{\left(i^2\cdot q2_j\cdot\sin\left(\beta 2_j\right)\cdot\sin\left(\beta 3_{m,j}\right) + \cos\left(\beta 2_j\right)\cdot\cos\left(\beta 3_{m,j}\right)\cdot q3_{m,j}\right)}{q3_{m,j}}$$

Reflection coefficient: $r_{m,j} := \frac{\left(f00(m,j) + f01(m,j)\cdot q4_j\right)\cdot q1_j - \left(f10(m,j) + f11(m,j)\cdot q4_j\right)}{\left(f00(m,j) + f01(m,j)\cdot q4_j\right)\cdot q1_j + \left(f10(m,j) + f11(m,j)\cdot q4_j\right)}$

Reflection Ratio: $RTM_{m,j} := \overline{r_{m,j}}\cdot r_{m,j}$

References

Wilford N. Hansen. Journal of the optical society of America. Volume 58, Number3. Page 380-390

Max Born & Emil wolf. Principles of optics. Sixth Edition. Chapter 1.6.2

David J. Griffiths. Introduction to Electrodynamics. Second edition. Chapter 8.4.3

Charles Kittel. Introduction to solid State physics. Seventh Edition. Chapter 10

G. jungk and C.H. Lange, Phys. Status Solid (b) 50 (1972) K 71.